ELSEVIER

Journal of Molecular Catalysis A: Chemical 193 (2003) 13–20

JOURNAL OF MOLECULAR CATALYSIS A: CHEMICAL

www.elsevier.com/locate/molcata

Study of the active site and activation process of Ni-based catalyst for 1,3-butadiene polymerization using X-ray absorption and crystal-field spectroscopies

Gwanghoon Kwag [a,*], Jung Goo Lee [a], Hosull Lee [a], Sunghyun Kim [b,1]

[a] *Kumho Chemical Laboratories, Korea Kumho Petrochemical Co., P.O. Box 64, Yuseong, Taejon 305-600, South Korea*
[b] *Department of Chemistry, Bio/Molecular Informatics Center, Konkuk University, Seoul 143-701, South Korea*

Received 11 March 2002; received in revised form 31 May 2002; accepted 22 July 2002

Abstract

The catalytic activation process of the Ni-based Ziegler–Natta catalyst composed of Ni(naphthenate)$_2$, catalytic amount of 1,3-butadiene, $BF_3{\cdot}OEt_2$ and $AlEt_3$, is spectroscopically observed by using synchrotron X-ray absorption and crystal field spectroscopies, and an optimum model of the nickel active site is proposed with the density functional theory (DFT) calculations. In the X-ray absorption near edge structure (XANES) spectrum of nickel naphthenate (NN), the position of the pre-edge at 8330.0 eV and both the strong edge and the weak pre-edge peaks indicate that NN possesses high O_h symmetry and is in a divalent state. The similar XANES spectra of NNB (the mixture of NN and catalytic amount of 1,3-butadiene) and NNBF (the mixture of NNB and $BF_3{\cdot}OEt_2$) indicate that 1,3-butadiene and $BF_3{\cdot}OEt_2$ do not greatly disturb the coordination geometry around nickel. $AlEt_3$ functions as the alkylating agent in the presence of $BF_3{\cdot}OEt_2$, and initiates 1,3-butadiene polymerization in NNBFA (the mixture of NNBF and $AlEt_3$) where the coordination geometry is altered from O_h- to T_d-like but nickel remains in a divalent oxidation state. In the absence of $BF_3{\cdot}OEt_2$, $AlEt_3$ works as the reducing agent in NNBA (the mixture of NNB and $AlEt_3$). A single and well-defined peak at 1.62 Å is observed for NN due to the Ni–O shell in the phase-uncorrected Fourier-transformed (FT) EXAFS (extended X-ray absorption fine structure) spectrum of NN. A significant change in the EXAFS spectrum of NNBFA has occurred where the main peak shifts toward a higher distance with increased complexity. The complex nature of the peak at 1.75 Å indicates that the coordination feature around nickel differs from the Ni–O shell and the longer bonds, Ni–C and Ni–F, are formed. The Ni–F bond of NNBFA is confirmed by the Ni–F peak, −137 ppm, in the ^{19}F-NMR spectrum. The three main absorption bands, around 8830, 14660 and 24940 cm^{-1}, are obtained with the crystal field spectra of NN, NNB and NNBF, which represent a typical octahedral structure of Ni(II) having three spin-allowed transition bands from $^3A_{2g}$ ground state to the $^3T_{2g}$, $^3T_{1g}$(F) and $^3T_{1g}$(P) states, respectively. Heterogeneity of the Ziegler–Natta catalyst is evidenced by strong scattering in the UV-Vis region of NNBFA.

Keywords: Ziegler–Natta catalyst; 1,3-Butadiene polymerization; Active site; X-ray absorption spectroscopy; Crystal field spectroscopy

1. Introduction

Nickel-based catalysts for the Shell Higher Olefin Process (SHOP), hydrogenation, 1,3-butadiene

* Corresponding author. Fax: +82-42-862-5651.
E-mail address: gkwag@kkpc.com (G. Kwag).
[1] Co-corresponding author.

1381-1169/02/$ – see front matter
PII: S1381-1169(02)00479-X

polymerization, and α-olefin polymerization have drawn both academic and industrial interest due to their unique mechanistic pathways in comparison with early transition metals [1–7]. Among them, the most notable example is the nickel-based Ziegler–Natta catalyst for 1,3-butadiene polymerization, composed of Ni(naphthenate)$_2$, catalytic amount of 1,3-butadiene, $BF_3{\cdot}OEt_2$ and $AlEt_3$ [8]. The polybutadiene produced with this catalyst has 96%-*cis* 1,4-content and possesses a high molecular weight with a broad molecular-weight distribution [3b]. The nature of the active site and the functions of cocatalysts are, however, still in dispute [9,10]. In the unique quaternary catalyst system, polymerization activity and the active sites are varied by the combination of alkylaluminum and $BF_3{\cdot}OEt_2$ [3], whereas in many other nickel-based catalysts activity is controlled by alkylaluminum alone [1,2,4–7].

Serious limitations to studying the active site are the lack of crystallinity, multi-active sites, and low stability. In the present study, we employed synchrotron X-ray absorption and crystal field spectroscopic techniques to overcome such limitations, and describe our spectroscopic findings for the two different functions of alkylaluminum and the structure of the nickel-based active site.

2. Experimental

2.1. Materials

$BF_3{\cdot}OEt_2$, $AlEt_3$ and 2,2,6,6-tetramethyl-3,5-heptanedione were purchased from Aldrich or Lancaster Chemicals. Nickel fluoride and nickel naphthenate (5.0%) were purchased from Strem Chemicals and Dainippon Ink, respectively.

2.2. Synthesis of $NiF_2((CH_3)_3CCOCH_2COC(CH_3)_3)_2$

A mixture of NiF_2 (5.0 g, 0.052 mol) and 2,2,6,6-tetramethyl-3,5-heptanedione (20.0 g, 0.11 mol) in butyl ether was refluxed for 5 h, and evaporated to dryness. The resulting liquid was chromatographed (BioBeads, S-X12). ^{19}F NMR(C_6D_6, 188 MHz, $CFCl_3$): −139 ppm. ^1H NMR(C_6D_6, 200 MHz): 1.07 (m), 5.70 (s), 16.91 (s).

The liquid is dark reddish brown. It is soluble in cyclohexane and toluene.

2.3. Catalyst preparation and XAS cell

The active Ziegler–Natta catalyst for XAS experiments, was prepared under nitrogen, by mixing Ni(naphthenate)$_2$ (1.20 mmol, 12% in toluene), butadiene (2.80 mmol), $BF_3{\cdot}OEt_2$ (13.0 mmol, 1.0 M in toluene) and $AlEt_3$ (6.10 mmol, 1.0 M in toluene) in order. The catalyst was rapidly frozen at −78 °C, and then placed in an air-tight XAS cell under N_2 atmosphere. The cell was made of Teflon with two Mylar windows (1/2000 in.; window size, 20 mm × 8 mm; optical path length, 2 mm), Fig. 1.

2.4. XAS measurement and data analysis

Nickel K-edge XAS measurement was carried out using Beam Line 3-C (2.0 GeV; 80–150 mA; Si(1 1 1) double flat crystal monochromator) at the Pohang Accelerator Laboratory (PAL) at POSTECH, Korea. XAS data were collected at room temperature in the transmission mode using $N_2(I_0)$ and Ar(I) filled ionization detectors. The monochromator was detuned by 30% in incident X-ray beam. All of data were internally calibrated using a Ni foil (8333.0 eV). The near-edge region was scanned at equal energy step of 0.30 eV per point to resolve fine structures. The EXAFS spectra were obtained at constant wave vector k, 0.05 Å^{-1}. The primary XAS data, $\ln(I_0/I_t)$, were normalized after extending the pre-edge region to the post-edge region using the Victoreen formula. EXAFS was extracted from the normalized XAS spectra after converting from electron volts to wave-vector (k) by the equation, $k = [0.263(E - E_0)]^{1/2}$, and fitting with a routine (AUTOBK) provided in the UWXAFS package (version 3.0). The EXAFS, $\chi(k)$, is described by the following equation,

$$\chi(k) = \sum_R N_R S_0^2 \frac{f_{\text{eff}}}{kR^2} \sin(2kR + \phi(k)) \exp(-2k^2\sigma^2) \times \exp\left(-\frac{2R}{\lambda}\right)$$

The parameter of our primary interest is the interatomic distance, R. We multiplied $\chi(k)$ by k^3 to enhance the oscillatory part at high k.

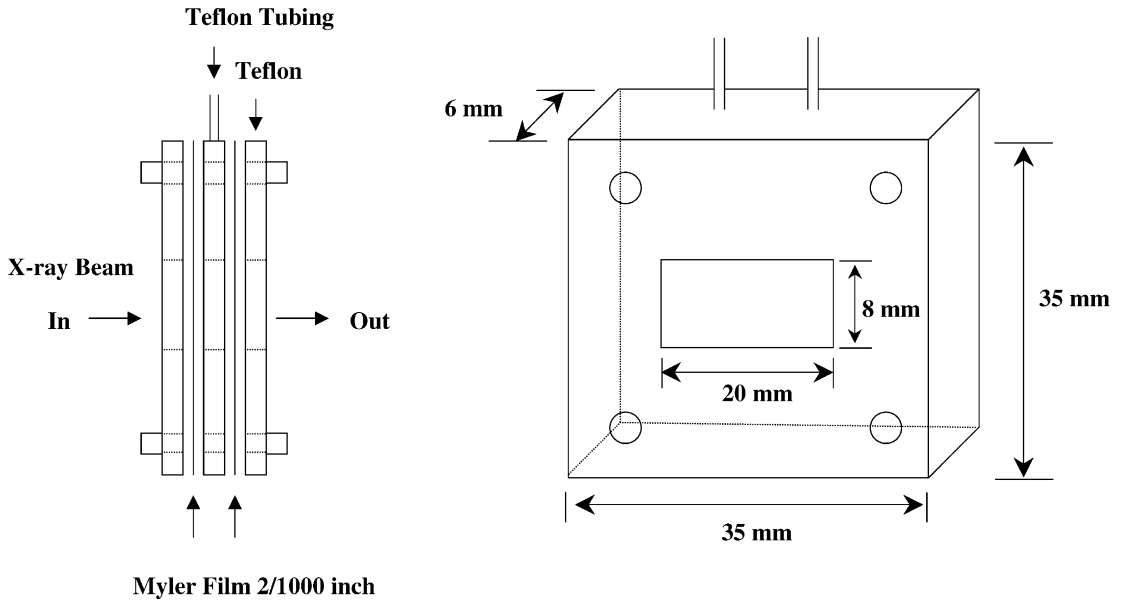

Fig. 1. XAS Cell for liquid and air-sensitive catalyst.

2.5. Other spectroscopic measurements

The crystal field spectra were obtained in an air-tight quartz cell with a JASCO V-570 UV-Vis–NIR spectrophotometer at room temperature. For the crystal field measurement Ni(naphthenate)$_2$, $BF_3{\cdot}OEt_2$, and $AlEt_3$ was diluted in toluene. ^1H and ^{19}F NMR spectra were recorded on a Varian Unity Plus 200-NMR spectrometer operated at 200 and 188 MHz, respectively. ^{19}F NMR chemical shifts are relative to $CFCl_3$ as an external reference. Matrix-assisted laser desorption ionization (MALDI) mass spectra were obtained from Korea Basic Science Institute (matrix = 2, 5-dihydroxy benzoic acid).

3. Results and discussion

3.1. XANES study

The active catalyst, NNBFA, for XAS experiments was prepared by mixing Ni(naphthenate)$_2$ (NN), catalytic amount of 1,3-butadiene, $BF_3{\cdot}OEt_2$ and $AlEt_3$, and polymerized 1,3-butadiene as shown in Scheme 1.

NN is a mixture of nickel aliphatic carboxylates, highly soluble in non-polar solvent and green in toluene. From the MALDI mass spectrum of NN, its major molecular weights (m/z) are 1269.2, 1205.54, 1057.7, 844.3, 785.6, 576.4 and 365.1. Since no crystal structure of NN is available, nickel aceate tetrahydrate

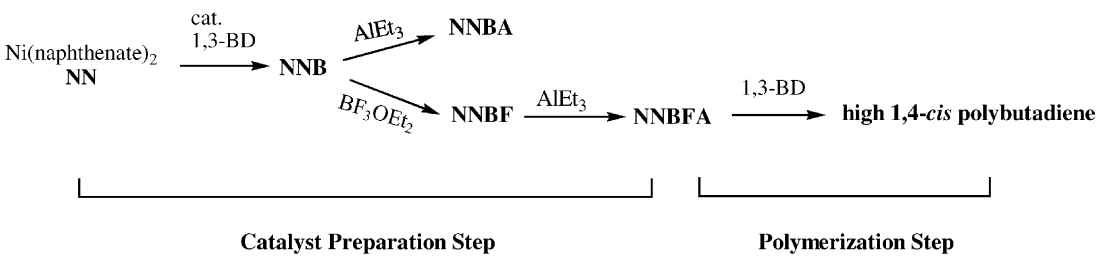

Scheme 1. Catalyst activation steps of the nickel-based Ziegler–Natta catalyst for 1,3-butadiene polymerization.

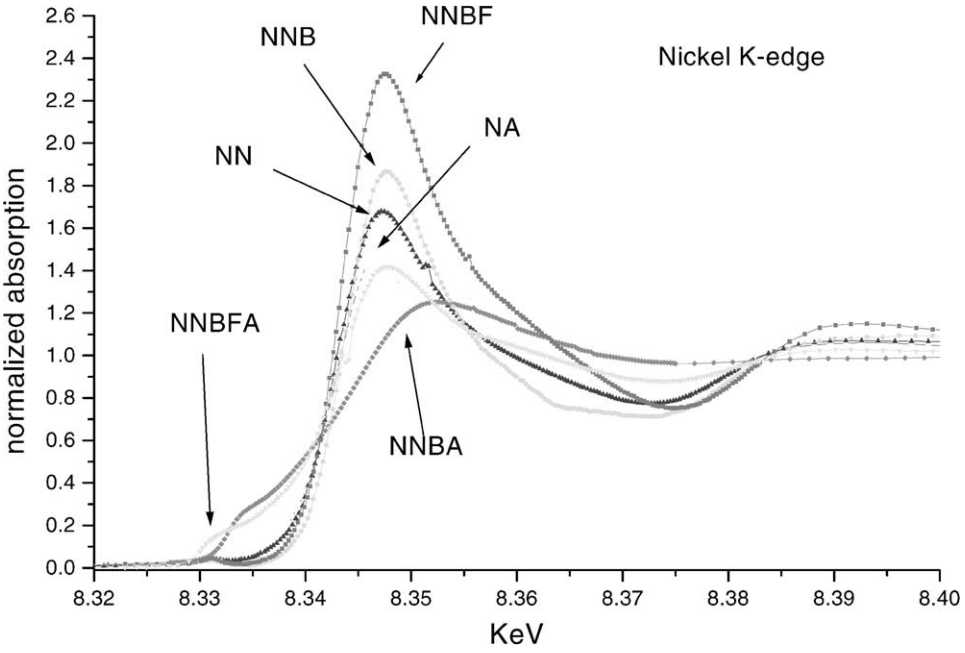

Fig. 2. Ni K-edge XANES spectra of NA, NN, NNB, NNBF and NNBFA.

(NA), which possesses O_h symmetry with 6 oxygen ligands, is employed as the reference for the structural study. Fig. 2 shows the evolvement of normalized XANES spectra of nickel K-edge. The positions of the pre-edges of NN, NNB, NNBF and NNBFA are located at 8330.0 eV, which are the same as that of NA. This result indicates that nickel is in the +2 state during the entire activation process. The pre-edge peak, due to dipole-forbidden but quadruple-allowed transition of 1s → 3d, is also an indication of site symmetry around nickel(II). The weak intensity of NN, NNB and NNBF implies that nickel is surrounded by an octahedron of six oxygen atoms, resulting in minimal orbital hybridization. This result is confirmed in comparison with that of NA, and implies that 1,3-butadiene and $BF_3{\cdot}OEt_2$ are located such a long distance from nickel and thus they do not greatly disturb nickel coordination sphere. A large change was observed in NNBFA where $AlEt_3$, forming the Ni–C bond and initiating polymerization, was added to NNBF. The large reduction of the main absorption peak, the relative enhancement of the pre-edge peak and the absence of splitting of the main-edge slope indicate that the symmetry changed from O_h-to T_d-like [11]. The lowering of the symmetry causes an increase in orbital mixing between the 3d and 4p nickel orbitals and in overlap of the 3d nickel orbitals with the 2p ligand orbitals. Since a new coordination site for butadiene should be needed after the activation step for polymerization to occur, the coordination geometry around nickel is to be altered from the highly saturated and strongly coordinated geometry.

The XANES spectrum of NNBA (the mixture of nickel naphthenate, butadiene and $AlEt_3$) is similar to that of Ni foil or Raney Nickel, in which K-edge peak is located at 8333 eV [12]. In the absence of $BF_3{\cdot}OEt_2$, the reduction of nickel to the zero valent state is observed. This observation indicates that $AlEt_3$ functions not only as an alkylating agent but also as a reducing agent for nickel. This arises from the formation of a highly unstable nickel dialkyl, which decomposes to metallic nickel. The reduced metallic nickel loses its catalytic activity for 1,3-butadiene polymerization. This supports that BF_3 is involved in the active center of 1,3-butadiene polymerization, where fluorine increases *cis* content by promoting the electron deficiency of nickel with consequently stronger η^4-*cis* coordination of butadiene [3].

3.2. Crystal field study

Another structural study was carried out using visible-near IR spectroscopic techniques, which would provide crystal field information around nickel. Four main absorption bands, around 8830, 13370, 14660 and 24940 cm^{-1}, were obtained with NN, NNB and NNBF solutions in the visible and near infrared region, Fig. 3. In a typical octahedral structure, Ni(II) has three spin-allowed transition bands, from $^3A_{2g}$ ground state to the $^3T_{2g}$, $^3T_{1g}$(F) and $^3T_{1g}$(P) states, corresponding to 8830, 14660 and 24940 cm^{-1}, respectively [13]. The transition energy of $^3A_{2g} \rightarrow {}^3T_{2g}$ corresponds to the crystal field splitting energy of the octahedral structure. In the visible region, a strong scattering was observed in NNBF or NNBFA sample due to insufficient homogeneity. We determined from the crystal spectra of NN, NNB and NNBF that 1,3-butadiene and $BF_3{\cdot}OEt_2$ barely disturbed the nickel coordination shell. In a regular tetrahedral structure, three major bands are observed around 5000, 8500 and 15000 cm^{-1}, which corresponds to spin-allowed transitions from $^3T_1(^3F)$ ground level to $^3T_2(^3F)$, $^3A_2(^3F)$, and $^3T_1(^3P)$ levels, respectively [14]. We could not observe any strong bands due to strong scattering but an weak absorption near 5000 cm^{-1} arose in NNBFA. This result strongly indicates multi-site and heterogeneous active species are formed.

3.3. Extended X-ray absorption fine structure (EXAFS) study

Further detailed information on the active site and nickel geometry was obtained from EXAFS spectra. Fig. 4 shows phase-uncorrected Fourier-transformed (FT) spectra of k^3-weighted EXAFS for a series of catalyst activation steps. As expected from the XANES, any noticeable change in peak positions was not observed in FT spectra until $AlEt_3$ was added. A single and well-defined peak at 1.62 Å observed for NN is due to the Ni–O shell. This peak is not much changed when $BF_3{\cdot}OEt_2$ and butadiene are added except for a shoulder at a rising part, indicating that $BF_3{\cdot}OEt_2$ and butadiene only weakly interact with nickel (see FT spectrum of NNBF). The curve fitting on the basis of the crystal data of NA and using UWXAFS 3.0 gives 2.03 ± 0.02 Å for the Ni–O distance.

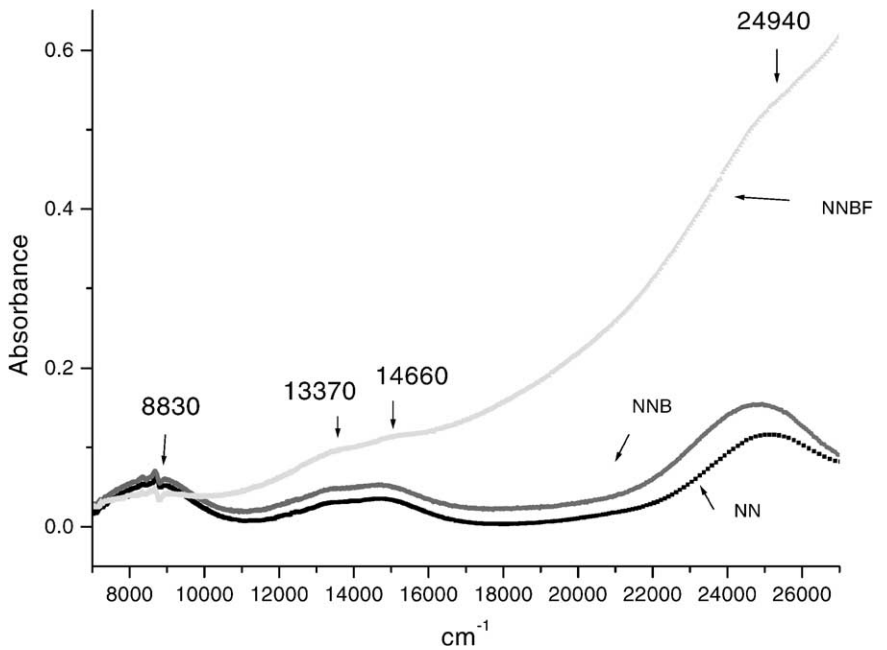

Fig. 3. Crystal field spectra of NA, NN, NNB and NNBF.

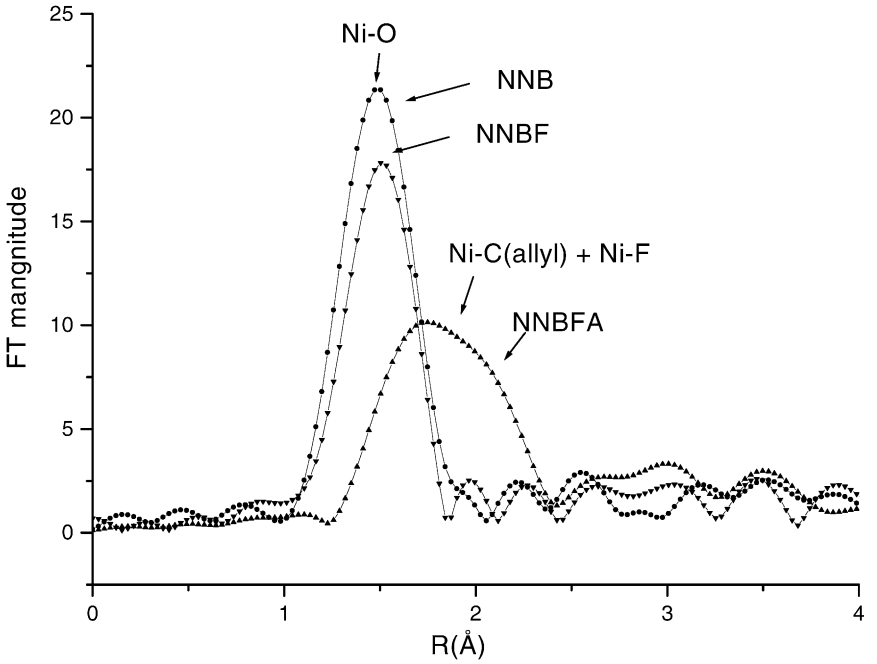

Fig. 4. Fourier transforms of EXAFS spectra of NN, NNBF and NNBFA (k range of 2–12 Å^{-1}).

A dramatic change in the EXAFS has occurred in NNBFA. The shift of the main peak takes place toward a higher distance with increased complexity. The complex nature of the peak at 1.75 Å indicates that the coordination feature around nickel differs from the Ni–O shell and the longer bonds, Ni–C and Ni–F, are formed. In accordance with the XANES and the crystal field spectra, $AlEt_3$ alters the coordination geometry and distances. The Ziegler–Natta catalyst consists of multi-active sites and many atoms are located at similar distances, contributing to the EXAFS spectrum. Therefore, curve fitting cannot simply distinguish all these contributions.

3.4. Proposed active site

The formation of Ni–F bond in NNBFA was monitored by ^{19}F NMR spectroscopic techniques

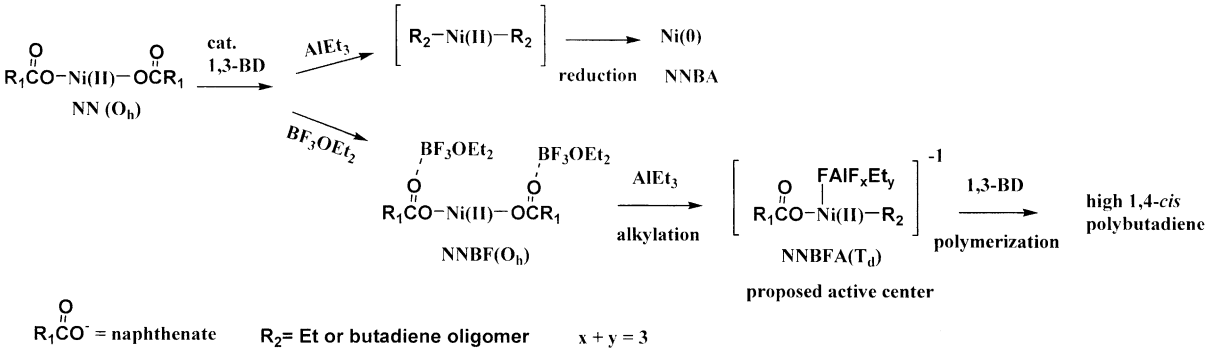

Scheme 2. Nickel structures during activation steps and a proposed active center.

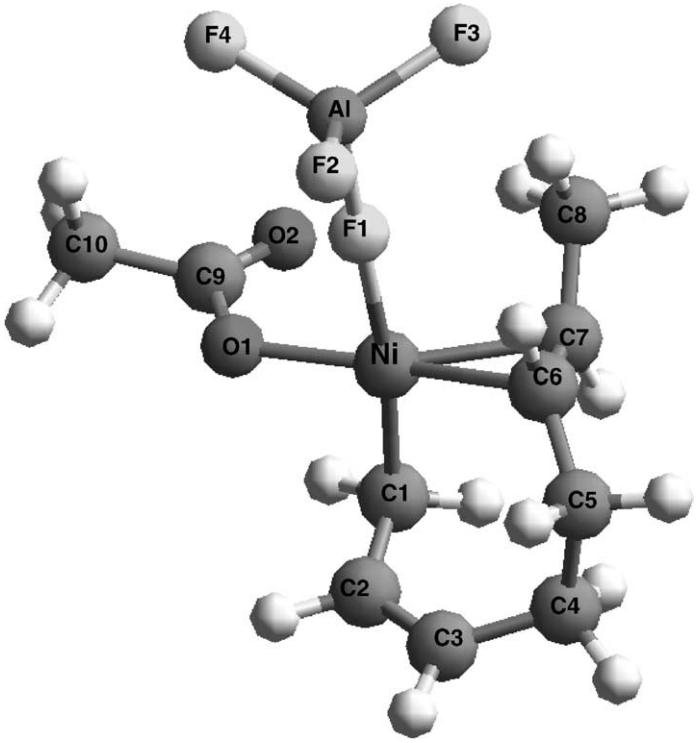

Fig. 5. Model of an active site of the nickel-based Ziegler–Natta catalyst for 1,3-butadiene polymerization (Ni–C_1 1.937 Å, Ni–C_6 2.151 Å, Ni–C_7 2.112 Å, Ni–F_1 2.044 Å, Ni–O_1 1.888 Å, Ni–O_2 3.019 Å, C_1–C_2 1.477 Å, C_2–C_3 1.360 Å, C_6–C_7 1.393 Å, F_1-Al_1 1.763).

(−137 ppm, standard $CFCl_3$ in C_6D_6) [15]. The Ni–F bond formation is also confirmed by the ^{19}F NMR spectrum of the model compound $NiF_2 \cdot ((CH_3)_3CCOCH_2COC(CH_3)_3)_2$ where the peak of Ni–F is located at −139 ppm. The data support that BF_3 works as a F-donor to form a Ni–F bond from NN by the ligand-exchange reactions with $BF_3 \cdot OEt_2$ and $AlEt_3$ as follows:

$$Ni(OOCR)_2 + AlEt_3 \rightarrow EtNi(OOCR) + RCOOAlEt_2 \quad (1)$$

$$EtNi(OOCR) + BF_3 \cdot OEt_2 \rightarrow FNi(OOCR) + BEtF_2 \cdot OEt_2 \quad (2)$$

We summarized these spectroscopic results as shown in Scheme 2, and built a three-dimensional model of an active site in which nickel(II) is coordinated with acetate, allylic active end with the penultimate double bond, and aluminum tetrafluoride. The DFT gradient calculations were then performed to determine the three-dimensional optimum geometry on the basis of the above results, using the Gaussian 94 program [16], where the hybrid method B3PW91 with the LanL2DZ basis set was employed. Fig. 5 shows an optimized geometry of the proposed active site, where the anti configuration of η^1-allyl ligand having the penultimate double bond is coordinated to Ni(II), and the polybutadiene propagation chain is geometrically distorted to maintain the *cis*-configuration.

4. Conclusions

Our aim of this work is to clarify functions of alkylaluminum and the nature of the nickel in the Zigler–Natta catalyst for 1,3-butadiene polymerization using synchrotron X-ray absorption and crystal field spectroscopies. Based on the XANES, EXAFS, crystal field structure and DFT calculations, the following

conclusions are reached: (1) alkylaluminum works as an alkylating agent in the presence of BF_3 and as a reducing agent in the absence of BF_3; (2) nickel remains in a divalent state during the entire activation processes in the presence of BF_3; (3) the geometrical change from O_h- to T_d-like structure around nickel occurs with the addition of alkylaluminum; (4) the Ni–F bond formation, which promotes *cis*-configuration of polybutadiene, takes place after the addition of $AlEt_3$; (5) DFT calculations suggest the formation of Ni(II)—η^1-allyl and Ni(II)—penultimate double bonds.

Acknowledgements

Experiments at Pohang Accelerator Laboratory were supported in part by MOST and POSCO.

References

[1] F.H. Kowalt, R. Goddard, C. Kruger, Angew. Chem. Int. Ed. Chem. 17 (1978) 466.
[2] J.J. Eisch, S.R. Sexsmith, K.C. Fichter, J. Organomet. Chem. 382 (1990) 273.
[3] (a) J. Furukawa, Acc. Chem. Res. 13 (1980) 1;
(b) M. Morton, Rubber Technology, Van Nostrand Reinhold, New York, 1987, p. 250.
[4] S.A. Svejda, L.K. Johnson, M. Brookhart, J. Am. Chem. Soc. 121 (1999) 10634.
[5] G.G. Arzoumanidis, N.M. Karayannis, CHEMTECH 7 (1993) 43.
[6] H.H. Brintzinger, D. Fischer, R. Mulhaupt, B. Rieger, R.M. Waymouth, Angew. Chem. Int. Ed. Engl. 34 (1995) 1143.
[7] T.R. Younkin, E.F. Connor, J.I. Henderson, S.K. Friedrich, R.H. Grubbs, D.A. Bansleben, Science 287 (2000) 60.
[8] (a) S. Kitagawa, Z. Harada, Jpn. Chem. Q. IV-1 (1967) 41;
(b) J. Furukawa, Pure Appl. Chem. 42 (1975) 495.
[9] (a) R. Taube, S. Wache, J. Organomet. Chem. 428 (1992) 431;
(b) J. Sieler, R. Kepe, S. Wache, R. Taube, J. Organomet. Chem. 455 (1993) 241;
(c) R. Taube, S. Wache, J. Sieler, J. Organomet. Chem. 459 (1993) 335;
(d) S. Wache, R. Taube, J. Organomet. Chem. 456 (1993) 137;
(e) R. Taube, J. Langlotz, G. Muller, J. Muller, Makromol. Chem. 194 (1993) 1273.
[10] (a) G. Kwag, Y. Jang, H. Lee, Polym. J. 31 (1999) 1274;
(b) H. Sato, Y. Yagi, Bull. Chem. Soc. Jpn. 65 (1992) 1299.
[11] (a) L. Galoisy, G. Calas, Mater. Res. Bull. 28 (1993) 221;
(b) L. Galoisy, G. Calas, Geochim. Cosmochim. Acta 57 (1993) 3613;
(c) L. Galoisy, G. Calas, Am. Miner. 77 (1992) 677.
[12] J. Rothe, J. Hormes, C. Schild, B. Pennemann, J. Catal. 191 (2000) 294.
[13] (a) G.R. Rossman, R.D. Shannon, R.K. Waring, J. Soild State Chem. 39 (1981) 277;
(b) H. Keppler, Am. Miner. 77 (1992) 75;
(c) M.L. Calatayud, I. Castro, J. Sletten, J. Cano, F. Lloret, J. Faus, M. Julve, G. Seitz, K. Mann, Inorg. Chem. 35 (1996) 2858;
(d) T. Yoshida, T. Suzuki, K. Kanamori, S. Kaizaki, Inorg. Chem. 38 (1999) 1059;
(e) M.J. Elejalde, R. Balda, J. Fernandez, J. Phys. 4 (1994) C4-411.
[14] L. Galoisy, G. Calas, J. Mater. Res. 6 (1991) 2434.
[15] D. Chen, J. Lian, Y. Yu, Y. Zhang, C. Zhong, X. Tang, Acta Polym. Sinica (1991) (4) 489.
[16] Gaussian 94, Revision D.3, by M.J. Frisch, G.W. Trucks, H.B. Schlegel, P.M.W. Gill, B. Johnson, G.M. Robb, A.J. Cheeseman, R.T. Keith, G.A.J. Peterson, A. Montgomery, K. Raghavachari, M.A. Al-Laham, V.G. Zakrzewski, J.V. Ortiz, J.B. Foresman, J. Cioslowski, B.B. Stefanov, A. Nanayakkara, M. Challacombe, C.Y. Peng, P.Y. Ayala, W. Chen, M.W. Wong, J.L. Andres, E.S. Replogle, R. Gomperts, R.L. Martin, D.J. Fox, J.S. Binkley, D.J. Defrees, J. Baker, J.P. Stewart, M. Head-Gordon, C. Gonzalez, J.A. Pople, Gaussian Inc., Pittsburgh, PA, 1995.